Available online at www.sciencedirect.com
SCIENCE DIRECT
Biochemical Pharmacology 69 (2005) 855–865
Biochemical Pharmacology
www.elsevier.com/locate/biochempharm

Mechanism of ricin-induced apoptosis in human cervical cancer cells

P.V. Lakshmana Rao[a,*], R. Jayaraj[a], A.S.B. Bhaskar[a], Om Kumar[a], R. Bhattacharya[a], Parag Saxena[b], P.K. Dash[b], R. Vijayaraghavan[a]

[a]*Division of Pharmacology and Toxicology, Defence Research and Development Establishment, Jhansi Road, Gwalior 474002, India*
[b]*Virology Division, Defence Research and Development Establishment, Jhansi Road, Gwalior 474002, India*

Received 6 September 2004; accepted 8 November 2004

Abstract

The mechanism of ricin-induced apoptosis in human cervical cancer cell line HeLa was studied. The present study demonstrated that ricin induces apoptosis of human cervical cancer cells (HeLa) in a time dependent manner with an IC_{50} for cell viability of 1 μg/ml. Ricin treatment resulted in a time dependent increase in LDH leakage, DNA fragmentation, percent apoptotic cells, generation of reactive oxygen species and depletion of intracellular glutathione levels. DNA agarose gel electrophoresis showed typical oligonucleosomal length DNA fragmentation. Additionally, DNA diffusion assay was performed to confirm DNA damage and apoptosis. Ricin activated caspase-3 as evidenced by both proteolytic cleavage of procaspase-3 into 20 and 18 kDa subunits, and increased protease activity. Caspase activity was maximum at 4 h and led to the cleavage of 116 kDa poly(ADP-ribose) polymerase (PARP), resulting in the 85 kDa cleavage product. Ricin-induced caspase-3 activation also resulted in cleavage of DNA fragmentation factor-45 (DFF45/ICAD) and DFF40 or caspase-activated DNase in HeLa cells. Activation of caspase-3, cleavage of PARP and DNA fragmentation was blocked by pre-treatment with caspase-3 specific inhibitor Ac-DEVD-CHO (100 μM) and broad-spectrum caspase inhibitor Z-VAD-FMK (40 μM). Ricin-induced DNA fragmentation was inhibited by pre-treatment with PARP inhibitors 3-aminobenzamide (100 μM) and DPQ (10 μM). Our results indicate that ricin-induced cell death was mediated by generation of reactive oxygen species and subsequent activation of caspase-3 cascade followed by down stream events leading to apoptotic mode of cell death.

Keywords: Ricin; HeLa cells; Apoptosis; Caspase-3; DNA fragmentation factor; Caspase inhibitors

1. Introduction

Ricin is a potent protein toxin isolated from the seeds of castor bean plant *Ricinus communis*. The ricin molecule is comprised of two glycoprotein chains A and B, of equal size (MW: ca. 62 kDa) that are joined by disulfide bond [1]. The B chain binds to galactose residues present on various cell surface glycoproteins and glycolipids and triggering endocytosis of toxin. The A chain reaches cytosol through Golgi complex after the reduction of the disulfide bond. Ricin A chain exhibits an RNA N-glycosidase activity which hydrolyses a specific adenine residue from a highly conserved loop region of 28S rRNA [2,3]. This RNA N-glycosidase activity results in loss of protein elongation and presumably subsequent death of the exposed cell. Ricin endocytosis may also occur through another recognition process which involves the interaction of mannose-containing carbohydrate side-chains of the toxin with mannose receptors. Ricin or it's A chain has been used to synthesize immunotoxins which show specific anti-cancer and anti-AIDS activities in vitro and in vivo [4].

Ricin is known to have diverse effects on cells of different organs like liver, kidney, pancreas, intestines and parathyroid [5]. The mechanisms of ricin toxicity

Abbreviations: Ac-DEVD-CHO, acetyl-Asp-Glu-Val-Asp aldehyde; Z-VAD-FMK, *N*-benzoyloxy-carbonyl-Val-Ala-Asp (*O*-me)-fluoromethyl ketone; GSH, glutathione; PARP, poly(ADP-ribose) polymerase; PMSF, phenylmethylsulfonyl fluoride; DTT, dithiothreitol; OPT, orthopthaldialdehyde; PBS, phosphate buffered saline; DCF-DA, 2,7-dichlorofluorescein diacetate; CHAPS, (3[(3-cholamidopropyl) dimethlylammonio]-1-propanesulfate); DFF/ICAD, DNA fragmentation factor/inhibitor of caspase-activated DNAse; CAD, caspase-activated DNAse

* Corresponding author. Tel.: +91 751 2341980; fax: +91 751 2341148.
E-mail address: pvlrao@rediffmail.com (P.V. Lakshmana Rao).

0006-2952/$ – see front matter © 2004 Elsevier Inc. All rights reserved.
doi:10.1016/j.bcp.2004.11.010

may include ribosome inactivation, disturbance in calcium-magnesium balance, release of cytokines, acute phase reactions, oxidative stress in the liver and apoptosis [3]. Ricin binds to cells, internalises through surface clathrin-coated pits into endosomes, and eventually translocates through intracellular membranes into the cytosol, where it irreversibly inactivates ribosomes inhibiting protein synthesis [6]. Ricin induces apoptosis in a wide variety of cells like bovine endothelial cells [7], MDCK cells [8] by mechanisms other than protein synthesis inhibition. Time and concentration dependent effects of ricin on some biomarkers of cellular toxicity including production of superoxide anion (O_2^-), nitric oxide, and DNA damage as well as cellular death have been examined in macrophage cell culture [9]. Ricin-induced hepatic lipid peroxidation, glutathione depletion and DNA single-strand breaks were reported by Muldoon et al. [10] in mice. We have recently reported ricin-induced oxidative stress associated hepatic and renal toxicity in mice [11].

Apoptosis is induced by a variety of stimuli, such as genotoxic compounds, toxins, tumour necrosis factor, various environmental stress. Cells undergoing apoptosis exhibit specific morphological changes, which include membrane blebbing, cytoplasm and chromatin condensation, nuclear breakdown, formation of apoptotic bodies eventually subjected to phagocytosis [12]. Caspases have emerged as the main players of the cell death programme, with apoptotic caspases been divided into executioner caspases (caspase-3, 6, 7) and initiator caspases (caspase-2, 8, 9, 10). Caspases initiate destruction of the nucleus, where a huge variety of different proteins are cleaved. By 2D-gel electrophoresis it has been recently determined that approximately 70 nuclear proteins are consistently degraded or translocated during apoptosis, irrespective of the cell type or apoptotic stimulus [13]. Recent studies have demonstrated that ricin induces cytotoxicity and apoptotic cell death in various cell types [14–16] but detailed mechanism is still unclear. To gain insight into mechanism of ricin-induced apoptosis in the present study, we investigated the role of oxidative stress and caspase-3 activation cascade in the apoptotic process in ricin-treated human cervical cancer (HeLa) cells.

2. Materials and methods

2.1. Materials

R. communis seeds used for ricin purification were obtained locally. HeLa cells were obtained from National Centre for Cell Science (NCCS), University of Pune. Proteinase K, RNAse, propidium iodide, GSH, caspase inhibitor peptides Ac-DEVD-CHO, Z-VAD-FMK, CHAPS, DTT, PMSF, were obtained from Sigma Chemical Co. 2,7-dichlorofluorescein diacetate, Hoechst 33342, OPT were purchased from Fluka. YOYO-1 was obtained from Molecular Probes. Low melting point agarose from BDH.

2.2. Ricin purification

Ricin was purified in the laboratory from *R. communis* seeds as described elsewhere [11]. Briefly, defatted castor seed meal was treated with 5% acetic acid and crude ricin was extracted. It was further purified by affinity chromatography performed on acid-treated Sepharose 4B (0.1 M HCl, 3 h, at 50 °C in 0.5 M sodium chloride solution) according to Griffiths et al. [17]. Under these conditions lectins bind to the gel matrix (to galactose residues available on the partially acid-hydrolysed matrix). The matrix bound proteins was eluted with β-D-galactose. These lectins were separated on the basis of their size difference using Bio-Gel® A-0.5m gel (Bio-Rad). The protein containing fractions were pooled separately, concentrated, and used for all experiments. PAGE under reduced and non-reduced conditions was performed each time to assess the purity of ricin.

2.3. Cell culture and treatment

HeLa cells (passage 104) obtained from NCCS, were grown in minimum essential medium (Eagle) without tryptose phosphate broth and supplemented with 2 mM L-glutamine, Earle's BSS adjusted to contain 1.5 g/L sodium bicarbonate, 0.1 mM non-essential amino acids, and 1.0 mM sodium pyruvate, 90%; fetal calf serum, 10% and gentamycin (80 μg/ml). Cells were maintained at 37 °C in a humidified atmosphere of 95% air and 5% CO_2 in a incubator. Viability of the cells was determined by Trypan blue dye exclusion. To study the effect of ricin on various parameters, HeLa cells were grown in serum free medium in either 24-well tissue culture plates or 25 mm^2 tissue culture flasks (Greiner) and treated with ricin (diluted in PBS) for different durations. The cells after treatment for specified duration were processed for various biochemical end points following procedures described below.

2.4. Cell viability assay

For IC_{50} determination HeLa cells were grown in (1–2×10^6 cells/well) in 24-well tissue culture plates and were exposed to various concentration of ricin for 12 h. The 50% inhibitory concentration (IC_{50}) of ricin was determined from the plots of viability of HeLa cells by crystal violet dye exclusion (CVDE) assay [18]. For all subsequent time course studies IC_{50} of ricin was used. Lactate dehydrogenase (LDH) activity in the culture media was measured spectrophotometrically as an index of plasma membrane damage and loss of membrane integrity [19]. Enzyme activity was expressed as the percentage of extra cellular LDH activity of the total LDH activity of the

cells. For time course studies on cell viability and LDH leakage treatment duration was 24 h.

2.5. Morphological determination of apoptosis

Following various treatments, apoptotic nuclei were quantified using fluorescence staining [20]. Briefly, at designated time points, media were removed and cells were washed once with PBS. The cells were then incubated with 10 μg/ml Hoechst 33342 (used to identify nuclear fragmentation) and 5 μg/ml propidium iodide (to identify non-viable cells) in PBS for 30 min at 37 °C. Cells were then visualized with fluorescence microscope (Carl Zeiss, Axiomot 2) and fragmented nuclei in viable cells were counted. For each treatment group, 800–1000 nuclei were counted. Data were expressed as percentage of viable cells with apoptotic nuclei.

2.6. DNA diffusion assay

DNA diffusion assay was done according to Singh [21] with slight modifications. Briefly, a layer of 0.5% low melting point (LMP) agarose was layered on a microslide and spread uniformly and dried at room temperature. Ten microlitres of either control or treated cell samples washed in PBS were mixed with 70 μl of 0.5% LMP agarose and layered on pre-coated slide. A cover glass was kept on the slide to get a uniform layering and cooled on a cold plate for 2 min. Cover glass was removed and 150 μl of 2% LMP agarose was layered above the previous layer and kept on cold plate. Lysis was done in a buffer containing 2.5 M NaCl, 2 mM tetrasodium-EDTA, 10 mM Tris base pH 10.0 with freshly added 1% Triton X-100 for 1 h at room temperature. After lysis, slides were kept in a freshly made solution containing 0.3 NaOH and 0.2% DMSO (pH > 13.5) for 10 min at room temperature. Slides were neutralized in 100 mM Tris–HCl pH 7.4 for 20 min. Slides were subsequently immersed in 5 mM spermine in 75% ethanol for 20 min. Staining was done in 1 μM of YOYO-1 in 2% DMSO and 0.5% sucrose. The nuclei were visualized under fluorescence microscope and photographed.

2.7. DNA fragmentation analysis

Quantitative analysis of DNA fragmentation was carried out as reported earlier [19]. The cells were lysed in ice-cold lysis buffer (10 mM Tris, 20 mM EDTA, 0.5% Triton X-100, pH 8.0) prior to centrifugation at 27,000 × *g* for 30 min. Both pellet (intact chromatin) and supernatant (DNA fragments) fractions were assayed for DNA content fluorimetrically. The percentage of DNA fragmented was defined as the ratio of the DNA content of the supernatant obtained at 27,000 × *g* to the total DNA in the lysate [22].

DNA fragmentation was qualitatively analysed by agarose gel electrophoresis [23]. Briefly, 2×10^6 cells were pelleted from the medium, washed once with Hank's balanced salt solution (HBSS), resuspended in 1 ml of HBSS, diluted with 10 ml of ice-cold 70% ethanol, and stored at −20 °C for 24 h. The cells were then pelleted by centrifugation (800 × *g* for 10 min) and ethanol was removed completely. The pellet was resuspended and the cells were lysed in 50 μl of phosphate–citrate buffer (192 parts of 0.2 M Na_2HPO_4 and eight parts of 0.1 M citric acid, pH 7.8). After incubation at room temperature for 30 min, the cell lysate was centrifuged (1000 × *g* for 5 min) and the supernatant was concentrated using a Speed Vac concentrator. A 5 μl 0.25% NP-40 in distilled water was added to each sample followed by 3 μl of RNAse A (1 mg/ml in water) and the suspension was incubated at 37 °C for 30 min followed by 5 μl of proteinase K (1 mg/ml) and incubated for further 30 min at 37 °C. DNA extracted from control and treated cells were electrophoresed on a 1.6% agarose gel impregnated with ethidium bromide. DNA ladder (1 kb; Promega) served as molecular size standard.

2.8. Measurement of intracellular ROS

Intracellular ROS was estimated using a fluorescent probe, 2,7-dichlorofluorescein diacetate (DCFH-DA). DCFH-DA diffuses through the cell membrane readily and is enzymatically hydrolysed by intracellular esterases to non-fluorescent dichlorofluorescin (DCFH), which is then rapidly oxidized to highly fluorescent DCF in the presence of ROS. Ricin was added at 1 μg/ml concentration simultaneously with DCFH-DA (final concentration 5 μM) and incubated at 37 °C up to 4 h. DCF fluorescence intensity was detected at different time intervals with excitation wave-length 485 nm and emission wavelength at 530 nm. The DCF fluorescence intensity is proportional to the amount of ROS formed intra-cellularly [24].

2.9. Measurement of intracellular GSH

Intracellular levels of GSH were determined using the method of Hisin and Hilf [25]. Cells after treatment were washed with PBS and scrapped into 6.5% trichloroacetic acid. Phosphate–EDTA buffer (4.5 ml) of pH 8.0 was added to 0.5 ml of 100,000 × *g* supernatant. The final assay mixture (2 ml) contained 100 μl of the diluted supernatant, 1.8 ml phosphate–EDTA buffer pH 8.0, and 100 μl *o*-phthalaldehyde solution containing 100 μg of OPT. After thorough mixing and incubation at room temperature for 15 min fluorescence was read at EM 420 and EX 350 nm in Shimadzu RF 5000 spectrofluorophotometer. The reduced form of GSH was used as a standard. Data were expressed as nanomole GSH per 10^6 cells.

2.10. Assay of caspase-3 activity

The activities of the caspase-3 like protease were measured in a fluorimetric assay modified from Nicholson et al.

[26]. After different treatments, cells were harvested with phosphate-buffered saline and centrifuged at 1500 rpm for 5 min. Cell pellets were resuspended in 2 ml buffer containing 59 mM Tris–HCl, 1 mM EDTA, 10 mM EGTA, and lysed with 10 μM digitonin. After incubation at 37 °C for 10 min, the lysates were centrifuged at 1000 × *g* for 5 min and the supernatants were stored at −70 °C till assayed. Protein concentration was estimated by Bio-Rad DC protein assay kit (Bio-Rad) and lysates (100 μg protein) were assayed in caspase assay buffer (312.5 mM HEPES (pH 7.5), 31.25% sucrose and 0.3125% CHAPS). The reaction was started with addition of 50 μM caspase-3 substrate, acetyl-Asp-Glu-Val-Asp aminomethylcoumarin (Ac-DEVD-AMC), and the reaction was followed for 60 min. Fluorescence was measured at excitation 360 nm and emission 460 nm in spectrofluorophotometer (Shimadzu RF 5000). Fluorescence intensity was calibrated with standard concentrations of AMC. Protease activity was calculated from the slope of the curve and expressed as pmol/min/mg protein.

2.11. Preparation of cell lysates for immunoblotting

For studies on caspase, DFF45/ICAD cleavage and DFF40/CAD, control and ricin-treated cells grown in 25 cm^2 tissue culture flasks were lysed in lysis buffer (10 mM HEPES pH 7.4, 42 mM KCl, 5 mM $MgCl_2$, 0.1 mM EDTA, 0.1 mM EGTA, 5 mM DTT, 2 mM PMSF, 1× complete protease inhibitor cocktail) containing 0.5% CHAPS. Cellular debris were spun down at 1440 × *g* for 20 min, and the supernatants were used as whole cell protein extracts. For PARP cleavage, cell extracts were prepared following the procedure of Shah et al. [27]. Briefly, Control and ricin-treated cells grown in 25 cm^2 tissue culture flasks were washed once with PBS, suspended at ∼5 × 10^6 cells/ml in sample buffer (6 M urea, 62.5 mM Tris–HCl, pH 6.8, 10% glycerol, 5% β-mercaptoethanol (freshly added), 2% SDS, 0.00125% bromophenol blue), sonicated for 15 s, and incubated at 65 °C for 15 min.

2.12. Western blotting analysis

Protein concentration of cell extracts was determined by Bio-Rad DC protein assay (Bio-Rad). Fifty micrograms protein from each sample was separated on SDS–PAGE and electrophoretically transferred onto a nitrocellulose membrane filter, using an electro-blotting apparatus (Bio-Rad). Membranes were incubated in blocking solution containing 5% non-fat dry milk in PBST buffer (PBS buffer containing 0.1% Tween-20) for 1 h at room temperature, followed by incubation for over night at 5 °C in platform shaker with various primary antibodies: monoclonal anti-PARP antibody at 1:2000 (clone C-2-10, Sigma) directed against uncleaved (116 kDa) and the cleaved form of PARP (85 kDa), anti-caspase-3, rabbit polyclonal antiserum (Calbiochem) recognizing whole caspase-3 (34 kDa) as well as large (20 kDa) and small sub units (18 kDa) diluted at 1:2000, and anti-DFF 45/ICAD, purified IgG fraction of polyclonal rabbit antiserum (Calbiochem) diluted to 1:2000 which recognizes uncleaved (45 kDa) and cleaved forms, and DFF40/CAD rabbit polyclonal IgG (Calbiochem) diluted to 1:2000. Monoclonal anti-β-actin (Clone AC-74, Sigma) which detects β-actin (42 kDa) is used as protein loading control. All antibodies are diluted in PBST with 5% milk powder. The membranes were washed four times in PBST for 15 min, followed by incubation for 2 h in horseradish peroxidase-conjugated rabbit anti-mouse or goat anti-rabbit secondary antibody (Dako) used at 1:150,000 dilution. The membranes were washed again and developed using an enhanced chemiluminescent detection system (ProteoQwest™ Chemiluminescent Western blotting kit, Sigma) according to manufacturer's protocol and the image was taken on Pierce CL-XPosure™ X-ray films.

2.13. Caspase and PARP inhibitor studies

For caspase-3 inhibition studies HeLa cells were pre-incubated with caspase-3 specific inhibitor, acetyl-Asp-Glu-Val-Asp-aldehyde (Ac-DEVD-CHO) at 100 μM and Z-VAD-FMK, 40 μM concentration 2 h prior to toxin treatment. The PARP inhibitors 3-amino-benzamide (100 μM) and DPQ {3,4-dihydro-5[4-(1-piperindinyl)butoxy]-1(2H)-isoquinoline} at 10 μM dissolved in DMSO were added to cells 2 h before ricin treatment. Cells were then incubated for 12 h. Inhibitor-treated cells were processed for DNA agarose gel electrophoresis and Western blot analysis for PARP cleavage.

2.14. Statistical analysis

Statistical analysis of the experimental data was carried out by Student's *t*-test. Values of $p \leq 0.05$ were considered to be significant, and results were expressed as mean ± S.E. of four replicates. Each experiment is repeated at least three times.

3. Results

3.1. Ricin-induced cytotoxicity

In order to determine the IC_{50} of ricin HeLa cells were treated with logarithmic concentration of ricin (1–10,000 ng/ml) in a 24-well tissue culture plate for 12 h and viability was determined by crystal violet dye exclusion assay. Ricin-induced a dose dependent decrease in viability with increasing concentration of ricin (Fig. 1) At 100 ng/ml viability was reduced to 63.4% and at 1000 ng/ml the viability was 51.0%. At 10 μg/ml viability was reduced to less than 10%. The IC_{50} was determined as

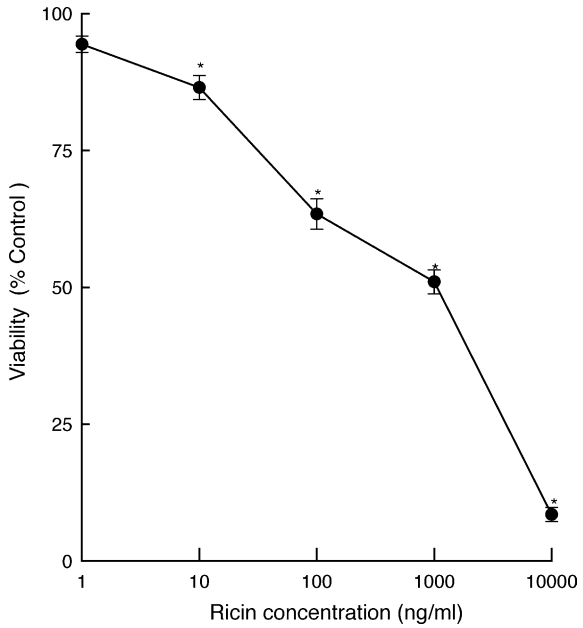

Fig. 1. Effect of ricin on viability of HeLa cells and determination of IC_{50}. HeLa cells (1×10^5 cells/well) grown in 24-well tissue culture plates were treated with logarithmic concentration of ricin for 12 h. The values are mean ± S.E. of four replicates. Significantly different from control at $^{*}p \leq 0.05$ by Student's *t*-test. Each experiment is repeated at least three times.

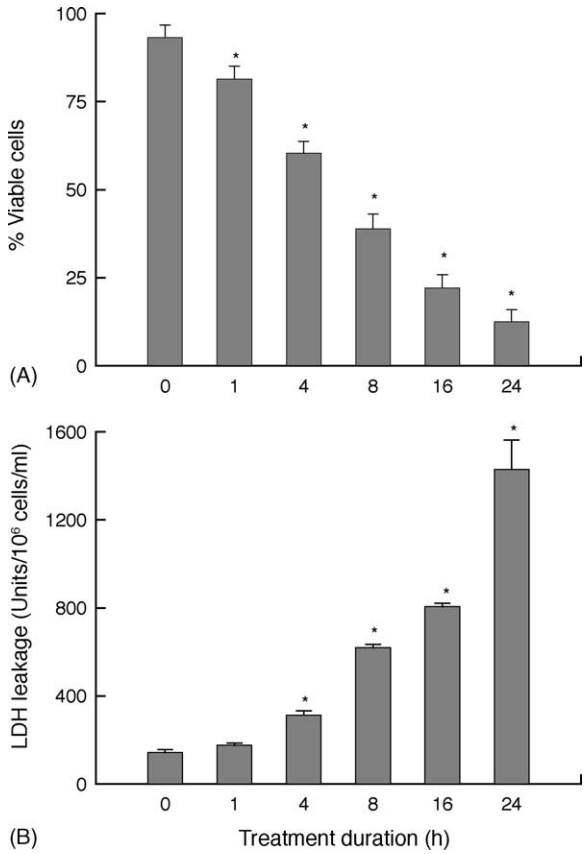

Fig. 2. Time course effect of IC_{50} of ricin (1 μg/ml) on viability of HeLa cells by CVDE assay (A) and LDH leakage (B). The values are mean ± S.E. of four replicates. Significantly different from control at $^{*}p \leq 0.05$ by Student's *t*-test.

1 μg/ml and for all subsequent experiments, the same concentration was used. Ricin-induced cytotoxicity was evaluated in a time course experiment by treating HeLa cells with 1 μg/ml of toxin and viability was determined by crystal violet dye exclusion and intracellular LDH leakage (Fig. 2A and B). There was no significant change in viability after 1 h treatment and viability was reduced to nearly 50% by 8 h. Marked morphological changes could be seen after 4–8 h characterized by plasma membrane blebbing, contraction of cell boundary or shrinkage of cells so that cell-to-cell contact in the originally confluent monolayer was lost. At 16 h there were fewer adherent cells and many of them were detached. The viability profile by intracellular LDH leakage also correlated well with CVDE assay. There was time dependent increase in LDH leakage after 4 h and reached maximum leakage by 24 h treatment.

3.2. Effect of ricin on apoptosis and DNA fragmentation

Ricin-treated HeLa cells (1 μg/ml) stained with Hoechst and propidium iodide exhibited morphological changes typical of apoptosis including cell shrinkage, plasma membrane blebbing, chromatin condensation and nuclear fragmentation as compared to control cells with prominent rounded nuclei and defined plasma membrane contours (Fig. 3A–D). Quantitative estimation of apoptotic cells induced by ricin was evaluated in time course experiment with 1 μg/ml for 24 h and the results are shown in Fig. 4A. At 1 h post-treatment there was no significant DNA fragmentation compared to control but a five-fold increase in apoptotic cells by 4 h (25.3 ± 4.1%). There was graded increase in number of apoptotic cells with treatment duration reaching maximum of 63.4% by 24 h. Quantitative DNA fragmentation profile of ricin-treated cells is shown in Fig. 4B. A time dependent increase in DNA fragmentation was observed with increase in treatment duration recording maximum fragmentation of 70.0% at 24 h treatment. In addition to quantitative DNA fragmentation qualitative fragmentation analysis was carried out by agarose gel electrophoresis. Ricin-treated cells showed typical internucleosomal DNA fragmentation or ''ladder'' formation at all time points tested (Fig. 4C). The intensity of banding was more prominent at 8, 16 and 24 h compared to earlier time points. DNA diffusion assay was done on ricin-treated cells to demonstrate the DNA fragmentation and also to identify cells undergoing death by apoptosis or necrosis. Control cells show a clear margins without any DNA diffusion and staining of the nucleus was intense (Fig. 5A and B). Apoptotic cell nuclei have a hazy or undefined outline without any clear boundary due to nucleosomal-sized DNA diffusing into agarose and necrotic cells have a larger halo with a clear boundary (Fig. 5C and D).

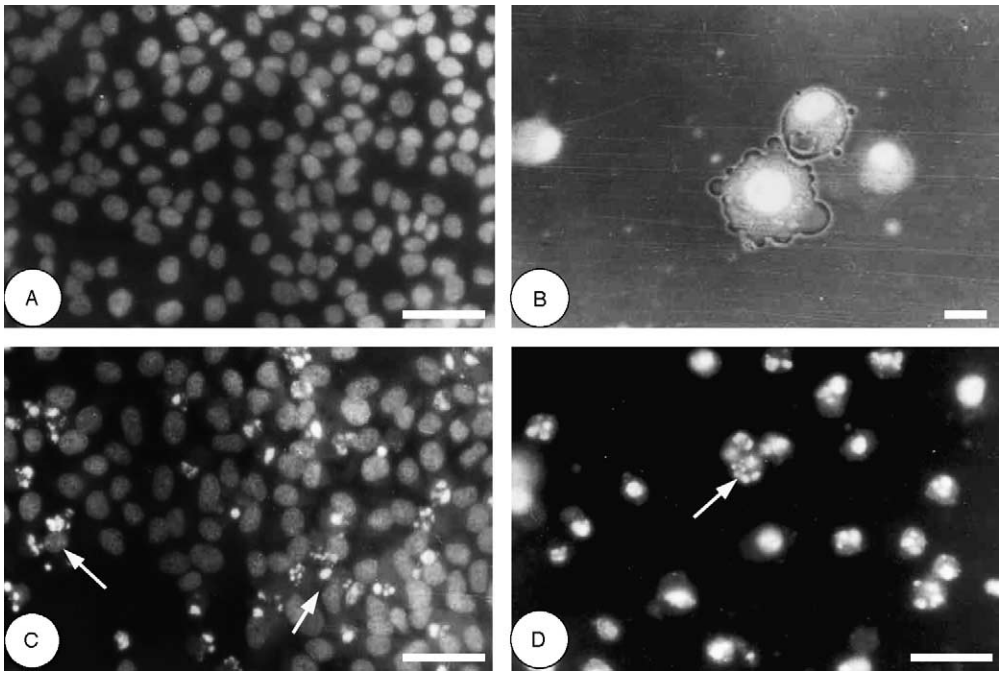

Fig. 3. Morphological features of ricin-induced apoptosis in HeLa cells treated with 1 μg/ml of ricin (A–D). (A) Fluorescence micrograph of control cells stained with HO-33342 showing normal nucleus. (B) Cells treated with ricin after 4 h showing plasma membrane blebbing. (C) Ricin-treated cells showing condensed chromatin (arrows). (D) Cells showing fragmented nucleus and apoptotic bodies (arrow). Scale bar 10 μm.

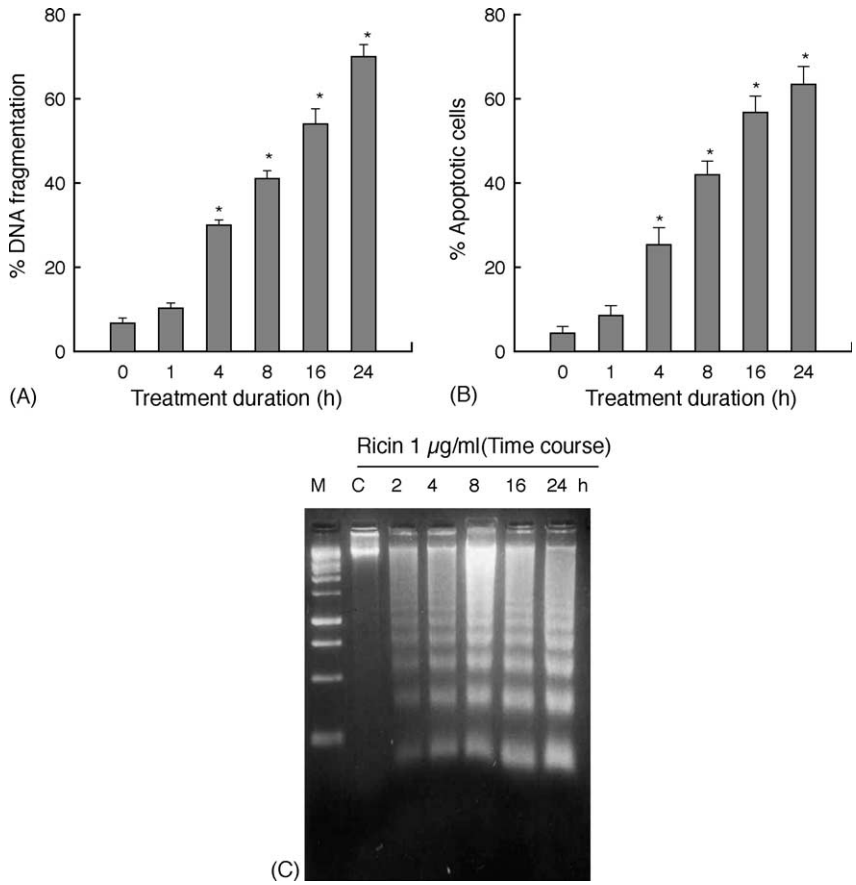

Fig. 4. Time course effect of 1 μg/ml of ricin on % DNA fragmentation (A) % apoptotic cells (B). The values are mean ± S.E. of four replicates. Significantly different from control at $^{*}p \leq 0.05$ by Student's *t*-test. (C) DNA agarose gel electrophoresis of ricin-treated HeLa cells (1 μg/ml) Lane M 1 kb ladder, lane 1 control, lanes 2–6 ricin-treated cells for 2, 4, 8, 16, 24 h, respectively.

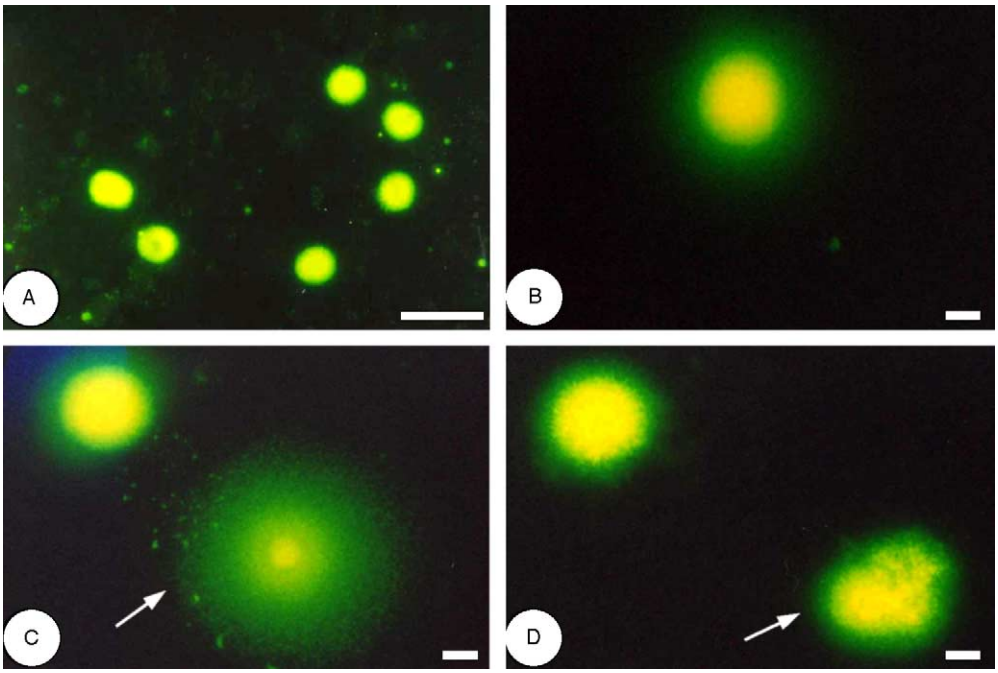

Fig. 5. DNA diffusion assay of control and ricin-treated HeLa cells after YOYO-1 staining (A–D). (A) and (B) control cells showing intensely stained nucleus. (C) A normal cell and an apoptotic cell (arrow) after ricin treatment for 8 h. (D) An early stage of necrotic cell (arrow). Scale bar: 5 μm.

3.3. Triggering of apoptosis by oxidative stress

Several reports suggest an involvement of reactive oxygen species (ROS), up stream of caspse-3 activation in signal transduction pathways leading to apoptosis. To determine the involvement of oxidative stress in ricin-induced HeLa cells apoptosis, ROS levels were determined in a time course experiment (Fig. 6A). Cells treated with ricin showed only marginal increase at 30 and 60 min post-treatment. At 2 h it showed nearly two-fold increase in levels compared to control cells. Maximum increase was observed at 3 h and no further increase was observed at longer treatment duration (data shown up to 4 h). One of the consequences of ROS is scavenging of free radicals by glutathione (GSH). Intracellular GSH levels were measured in ricin-treated HeLa cells at different time points and the results are summarized in Fig. 6B. There was significant GSH depletion in ricin-treated cells at 4 h with more than 50% depletion at 8 h and nearly 90% depletion compared to control cells at 24 h treatment.

3.4. Activation of caspase-3 and PARP cleavage

To directly address the involvement of caspase-3 like proteases in ricin-induced apoptosis, caspase-3 activity was determined in ricin-treated HeLa cells using fluorogenic caspase-3 substrate Ac-DEVD-AMC. Ricin-treated cells showed marginal caspase-3 activity by 1 h and reached three-fold increase by 4 h treatment (Fig. 7A). The casapase-3 activity reduced with treatment duration and reached a plateau by 8 h and no further increase was observed at 16 and 24 h treatment. The quantitative cas-

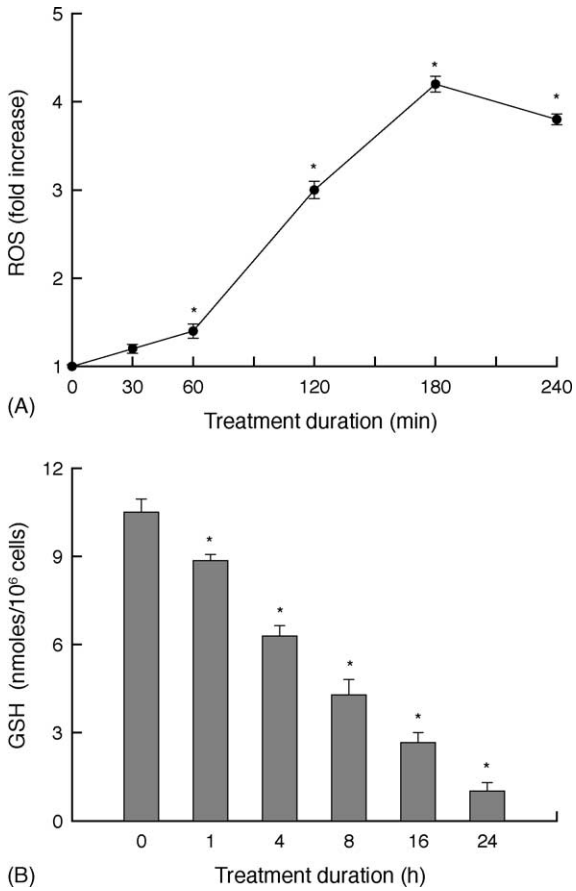

Fig. 6. Time course effect of 1 μg/ml of ricin on reactive oxygen species generation (A) and (B) intracellular glutathione levels. For ROS estimation cells were loaded with 5 μM DCF-DA followed by specified concentration of ricin and incubated at 37 °C for 4 h. The values are mean ± S.E. of four replicates. Significantly different from control at $^{*}p \leq 0.05$ by Student's *t*-test.

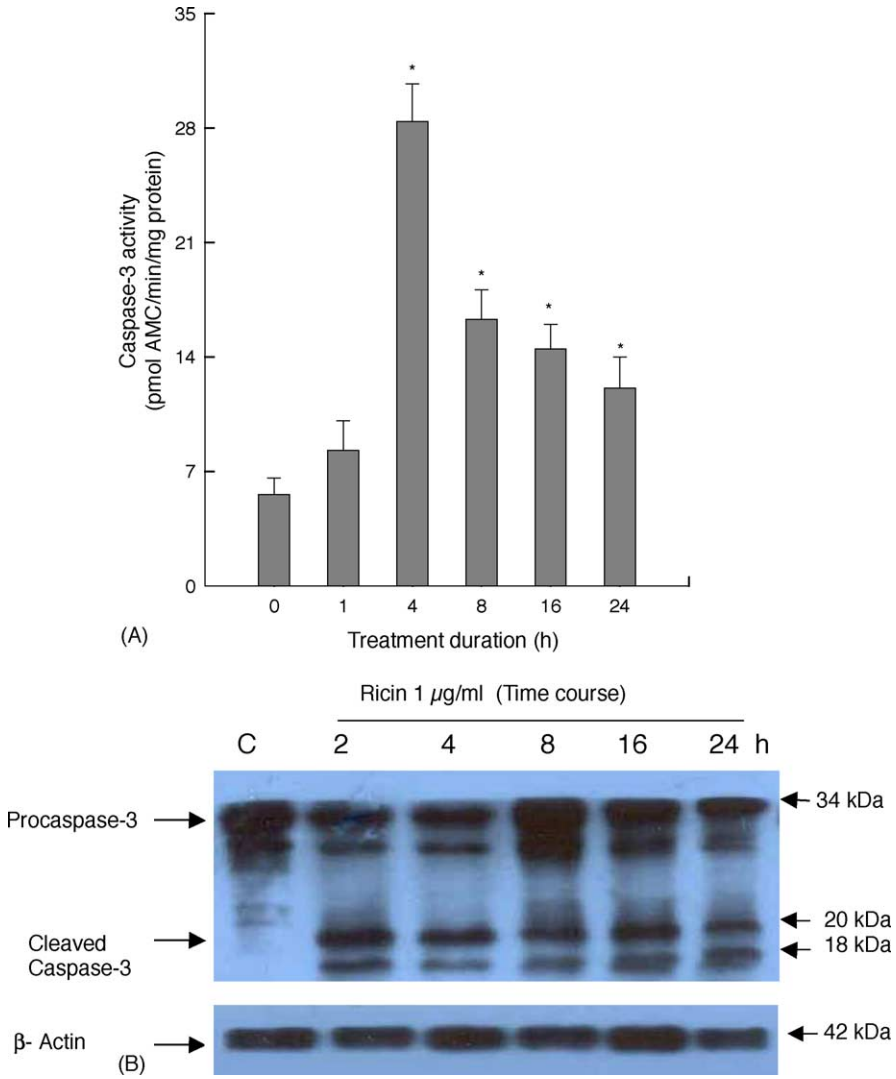

Fig. 7. (A) Time course effect of ricin 1 μg/ml on caspae-3 activity in HeLa cells. The values are mean ± S.E. of four replicates. Significantly different from control at $^{*}p \leq 0.05$ by Student's *t*-test. (B) Time course of procaspase-3 cleavage in HeLa cells in response to 1 μg/ml ricin. Blots showing procaspase-3 of 34 kDa and cleavage products of 20 and 18 kDa sub units. β-Actin is shown as protein loading control.

pase-3 activation after ricin treatment was confirmed with Western blot analysis. Fig. 7B shows uncleaved caspase-3 as 34 kDa band in control cells and cleaved products 20 and 18 kDa in ricin-treated samples at 2, 4, 8, 16 and 24 h time points.

Activation of caspase-3 leads to cleavage of number of proteins including PARP. Cleavage of PARP is an important indicator of apoptosis. Our results on Western blotting analysis of ricin-treated HeLa cells showed uncleaved 116 kDa and cleaved fragment of 85 kDa PARP (Fig. 8A). In addition to PARP cleavage, caspase activation leads to activation of DNA fragmentation factor (DFF) or ICAD. We evaluated the DFF/ICAD activity by Western blotting of ricin-treated cells harvested at 1, 2, 4, 8 and 16 h post-treatment. Our results show presence of DFF45/ICAD at 45 kDa at all time points. No cleavage was observed in control and 1 h time point but cleaved products in ricin-treated cells were observed at 2, 4, 8 and 16 h (Fig. 8B). Additionally, the same blots were stripped and probed with antibodies against DFF40/CAD. A band corresponding to CAD at 40 kDa was observed in 2, 4, 8 and 16 h treated samples and no bands were observed at control and 1 h.

3.5. *Effect of caspase and PARP inhibitors*

Effect of caspase-3 inhibitors on caspase-3 activity, PARP cleavage inhibition and DNA fragmentation was studied by pre-treating HeLa cells for 2 h with caspase-3 specific inhibitor Ac-DEVD-CHO (100 μM) and broad spectrum caspase inhibitor, Z-VAD-FMK (40 μM) prior to addition of 1 μg/ml ricin. As compared to ricin-treated cells, the caspase-3 activity was significantly reduced in cells pre-treated with caspase inhibitors (Fig. 9A). Even the morphology of inhibitor treated cells showed features similar to control cells with absence of plasma membrane blebbing, condensed chromatin and nuclear fragmentation

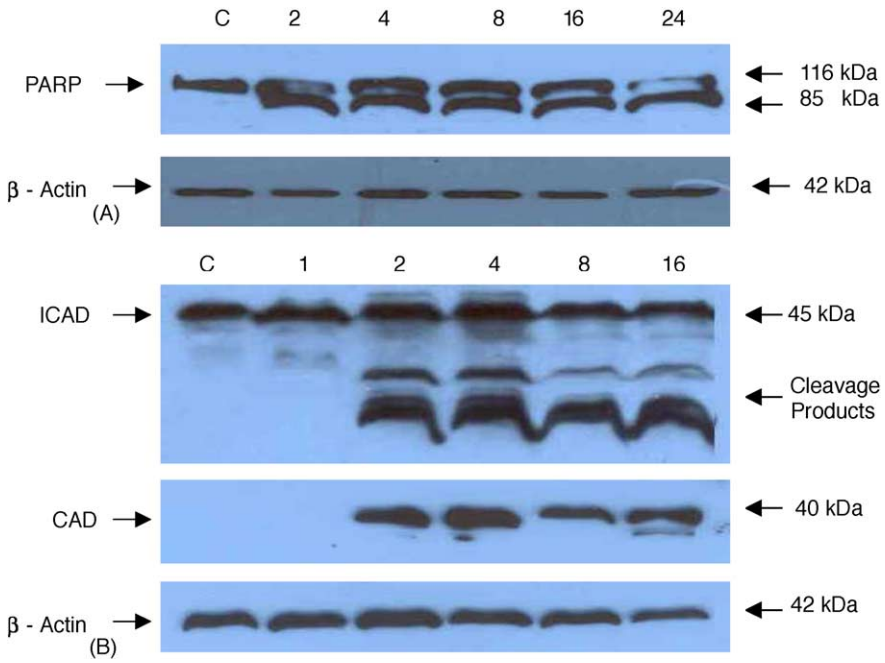

Fig. 8. (A) Time course of PARP cleavage in HeLa cells in response to 1 μg/ml ricin. (B) Time course of DFF45/ICAD and DFF40/CAD cleavage in HeLa cells in response to 1 μg/ml ricin. Upper panel shows DFF45 and its cleavage products after ricin treatment. β-Actin is shown as protein loading control.

(figures not shown). This quantitative data was confirmed with Western blotting analysis of PARP cleavage. For this study only representative time point of 8 h treatment duration was taken. Our results show inhibition of PARP cleavage into 85 kDa band and only 116 kDa uncleaved PARP could be observed in caspase inhibitor treated cells (Fig. 9B). In addition to Western blotting, DNA agarose gel electrophoresis of cells with and without caspase inhibitors

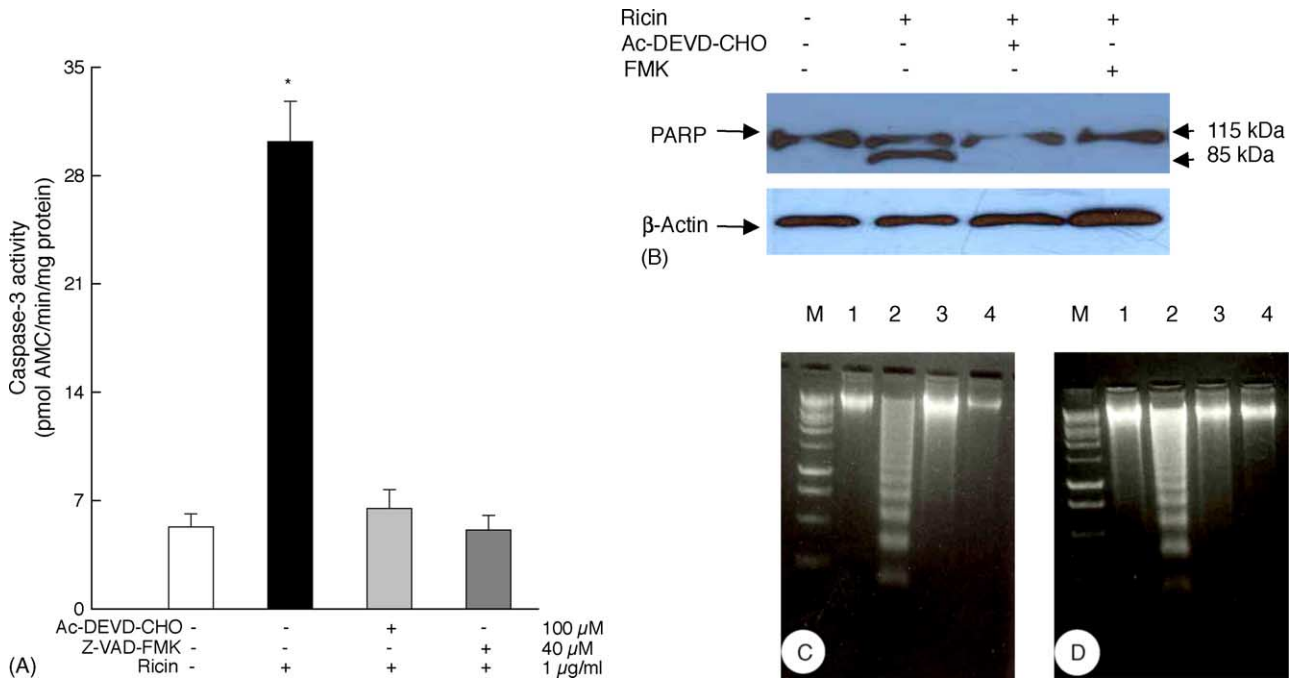

Fig. 9. Inhibition of ricin-induced caspase-3 activation and PARP cleavage by caspase inhibitors. (A) HeLa cells were pre-treated with Ac-DEVD-CHO (100 μM) and Z-VAD-FMK (40 μM) for 2 h before ricin treatment. Caspase activity was measured at maximum activation time point of 4 h. (B) Effect of caspase inhibitors on PARP cleavage. (C) Effect of caspase inhibitors on ricin-induced DNA fragmentation. Lane M 1 kb ladder: lane 1, control; lane 2, ricin 1 μg/ml; lane 3, Ac-DEVD-CHO (100 μM) + ricin 1 μg/ml; lane 4, Z-VAD-FMK (40 μM) + ricin 1 μg/ml. Representative of typical data of three experiments. (D) Effect of PARP inhibitors on ricin-induced DNA fragmentation. HeLa cells were pre-treated with PARP inhibitors for 2 h before ricin treatment. Lane M 1 kb ladder: lane 1, control, lane ricin 1 μg/ml; lane 3, 3-AB (100 μM) + ricin 1 μg/ml; lane 4, DPQ (10 μM) + ricin 1 μg/ml.

was carried out. There was complete blockage of internucleosomal DNA fragmentation in cells pre-treated with caspase inhibitors, Ac-DEVD-CHO and Z-VAD-FMK (Fig. 9C). We also evaluated the effect of PARP inhibitors 3-aminobenzamide (100 μM) and DPQ (10 μM) on DNA fragmentation by pre-treating HeLa cells with 3-AB and DPQ for 2 h prior to addition of ricin (1 μg/ml). Both the PARP inhibitors could not prevent completely ricin-induced DNA fragmentation (Fig. 9D).

4. Discussion

Ricin and related plant toxins belong to a group of enzymes called ribosome-inactivating proteins (RIP) [6]. In the present study, we investigated the mechanism of ricin-induced apoptosis in HeLa cells. Ricin-induced time dependent decrease in viable cells and increase in LDH leakage. Rounding of cells and plasma membrane blebbing could be seen initiated by 2–4 h. Drastic decrease in viability together with LDH leakage was noticed by 16–24 h treatment. Since under the in vitro cell culture conditions apoptotic cells cannot undergo rapid phagocytosis as in in vivo in the intact tissue, it might also be that LDH release is a feature of late apoptotic cells [28]. The quantitative data showed time dependent increase in percent apoptotic cells and percent DNA fragments. Conventional agarose gel electrophoresis and DNA diffusion assay confirm the ricin-induced DNA damage typical of apoptosis. But there are also reports of direct DNA damage induced by RIPs like ricin. Brigotti et al. [29] unequivocally showed that RIPs like ricin can damage nuclear DNA (by enzymatic activity) in human endothelial cell by means that are secondary to ribosome inactivation or apoptosis.

Ricin-treated HeLa cells showed significant increase in ROS generation. In the present study significant GSH depletion compared to control cells was also noticed in ricin-treated cells by 1 h and it depleted further by 4 h treatment. Ricin-induced GSH depletion was reported in other in vitro studies using different cell types. Oda et al. [8] used polarized MDCK cells to study the GSH efflux during ricin-induced apoptosis. Their results showed that when MDCK cells were pre-treated with Z-Asp-CH_2-DCB, a caspase family inhibitor inhibited ricin-induced basolateral GSH efflux as well as DNA fragmentation, suggesting that the activation of caspases, i.e. those that are inhibited by Z-Asp-CH_2-DCB, is implicated in the opening of the GSH transporter.

GSH depletion and direct oxidative damage are two different but related processes influencing the oxidation state of many proteins involved in the signal transduction pathways that regulate cell growth and death. Upon oxidative stress, GSSG may either recycle to GSH or exit from the cells leading to overall glutathione depletion. Depletion of reduced GSH commonly precedes or accompanies lipid peroxidation and oxidative stress. Recently, ROS production following GSH depletion has been demonstrated to represent a crucial event in the commitment to apoptosis in human B lymphoma cell line [30]. There is some debate as to whether apoptosis is triggered by a fall in GSH levels, or as increase in ROS or both. It is difficult to conclude from our limited experiments whether GSH depletion is preceded by oxidative stress or generation of ROS is responsible for GSH depletion.

Apoptosis is a central element in the pathogenesis of many disease processes and in the response to systemic therapies in neoplastic cells. Caspases have been identified as effectors of the apoptotic process and DNA fragmentation as well as nuclear morphological changes has been placed downstream of caspase activity [31,32]. The execution phase of apoptosis involves activation of caspases and the subsequent cleavage of several cellular substrates such as PARP, actin, fodrin, lamins, etc. The involvement of caspase in the death response to ricin in HeLa cells was evaluated by immunological detection of the 116 kDa of intact PARP and the appearance of its 85 kDa fragment, corresponding to product released upon activation of caspase. Our results support the earlier report by Gan et al. [33] on caspase-3 activation in ricin-induced apoptosis in HeLa cells. DNA fragmentation factor (DFF), also known as caspase-activated DNase (CAD) or caspase-activated nuclease has been implicated as the major nuclease responsible for DNA fragmentation [34–36]. DFF is composed of two subunits of 40 and 45 kDa, termed DFF40 (CAD) and DFF45 (ICAD) respectively [34]. Both DFF45 and its cleavage by caspase-3 are required for DNA fragmentation by DFF40 [37]. Results of our study show the involvement of CAD in the formation of nucleosomal length DNA fragmentation.

Pre-treatment of cells for 2 h with caspase-3 inhibitors Ac-DEVD-CHO and Z-VAD-FMK completely blocked ricin-induced PARP cleavage and DNA fragmentation. PARP inhibitors 3-AB and DPQ pre-treatment inhibited ricin-induced DNA fragmentation. PARP cleavage in apoptosis is thought to prevent ATP depletion by PARP over activation, preserving ATP and thus affording energy required for the active apoptotic process [38]. In conclusion, results of our present study shows that ricin-induced apoptosis in HeLa cells was associated with oxidative stress, glutathione depletion and activation of caspase-3 cascade followed by down stream events leading to apoptotic mode of cell death. Further studies are required to delineate the mechanism of ricin-induced oxidative stress and other triggers involved in signal transduction pathways associated with apoptosis.

Acknowledgment

The authors thank Mr. K. Sekhar, Director, DRDE and Dr. A.M. Jana, Head, Division of Virology, DRDE for providing facilities and critical suggestions.

References

[1] Olsnes S, Phil A. Different biological properties of two constituent peptide chain of ricin, a toxic protein inhibiting protein synthesis. Biochemistry 1973;12:3121–6.

[2] Endo Y, Tsurugi K. RNA N-glycosidase activity of ricin A-chain. J Biol Chem 1987;262:8128–30.

[3] Olsnes S. The history of ricin, abrin and related toxins. Toxicon 2004;44:361–70.

[4] Vitetta ES, Thorpe PE. Immunotoxins containing ricin or it's A chain. Semin Cell Biol 1991;2:47–58.

[5] Sadani GR, Soman CS, Deodhar K, Nadkarni GD. Reactive oxygen species involvement in ricin-induced thyroid toxicity in rat. Hum Exp Toxicol 1997;16:254–6.

[6] Barbieri L, Batteli MG, Stripe F. Ribosome-inactivating proteins from plants. Biochim Biophys Acta 1993;1154:237–82.

[7] Hughes JN, Lindsay CD, Griffiths GD. Morphology of ricin and abrin exposed endothelial cells is consistent with apoptotic cell death. Hum Exp Toxicol 1996;15:443–51.

[8] Oda T, Sadakata N, Komatsu N, Muramatsu T. Specific efflux of glutathione from the basolateral membrane domain in polarized MDCK cells during ricin-induced apoptosis. J Biochem 1999;126:715–21.

[9] Hassoun EA, Wang X. Time and concentration dependent production of superoxide anion, nitric oxide, DNA damage, and cellular death by ricin in the J774A.1 macrophage cells. J Biochem Mol Toxicol 1999;13:179–85.

[10] Muldoon DF, Hassoun EA, Stohs SJ. Ricin-induced hepatic lipid peroxidation, glutathione depletion and DNA single-strand breaks in mice. J Biochem Toxicol 1994;9:311–8.

[11] Kumar O, Sugendran K, Vijayaraghavan R. Oxidative stress associated hepatic and renal toxicity induced by ricin in mice. Toxicon 2003;41:333–8.

[12] Kerr JF, Wyllie AH, Currie AR. Apoptosis: a basic biological phenomenon with wide-ranging implications in tissue kinetics. Br J Cancer 1972;26:239–57.

[13] Gerner C, Gotzmann J, Frohwein U, Schamberger C, Ellinger A, Sauermann G. Proteome analysis of nuclear matrix proteins during apoptotic chromatin condensation. Cell Death Differ 2002;9:671–81.

[14] Griffiths GD, Leek MD, Gee DJ. The toxic proteins ricin and abrin induce apoptotic change in mammalian lymphoid tissues and intestine. J Pathol 1987;151:221–9.

[15] Komatsu N, Nakagawa M, Oda T, Muramatsu T. Depletion of intracellular NAD^+ and ATP levels during ricin-induced apoptosis through specific ribosomal inactivation results in cytolysis of U937 cells. J Biochem 2000;128:463–70.

[16] Tamura T, Sadakat N, Oda T, Muramatsu T. Role of zinc ions in ricin-induced apoptosis in U937 cells. Toxicol Lett 2002;132:141–51.

[17] Griffiths GD, Lindsay CD, Allenby AC, Bailey SC, Scawin JW, Rice P, et al. Protection against inhalation toxicity of ricin and abrin by immunisation. Human Exp Toxicol 1995;14:155–64.

[18] Wang CY, Mayo MW, Baldwin AS. TNF-α and cancer therapy-induced apoptosis: potentiation by inhibition of NF-κB. Science 1996;274:784–7.

[19] Rao PVL, Bhattacharya R, Parida MM, Jana AM, Bhaskar ASB. Freshwater cyanobacterium *Microcystis aeruginosa* (UTEX2385) induced DNA damage in vivo and in vitro. Environ Toxicol Pharmacol 1998;5:1–6.

[20] Rao PVL, Bhattacharya R, Nidhi G, Parida MM, Bhaskar ASB, Dubey R. Involvement of caspase and reactive oxygen species in cyanobacterial toxin anatoxin-a-induced cytotoxicity and apoptosis in rat thymocytes and Vero cells. Arch Toxicol 2002;76:227–35.

[21] Singh NP. A simple method for accurate estimation of apoptotic cells. Exp Cell Res 2000;256:328–37.

[22] Wyllie AH. Glucocorticoid-induced thymocytes apoptosis is associated with endogenous endonuclease activation. Nature 1980;284:555–6.

[23] Gong J, Trganos F, Darzynkiewicz Z. A selective procedure for DNA extraction from apoptotic cells applicable for gel electrophoresis and flow cytometry. Anal Biochem 1994;218:314–9.

[24] LeBel CP, Ischiopoulos H, Bondy SC. Evaluation of the probe 2,7-dichlorofluorescin as indicator of reactive oxygen species formation and oxidative stress. Chem Res Toxicol 1992;5:227–31.

[25] Hisin PJ, Hilf R. A fluorometric method for determination of oxidised and reduced glutathione in tissues. Anal Biochem 1976;74:214–26.

[26] Nicholson DW, Ali A, Thornberry NA, Vaillancourt JP, Ding CK, Gallant M, et al. Identification and inhibition of the IEC/CED-3 protease necessary for mammalian apoptosis. Nature 1995;376:37–43.

[27] Shah GM, Poirier D, Duchaine C, Brochu G, Desnoyers S, Laguenx J, et al. Methods for biochemical study of poly(ADP-ribose) metabolism in vitro and in vivo. Anal Biochem 1995;227:1–13.

[28] Grub S, Persohn E, Trommer W, Wolf A. Mechanisms of cyclosporine-A induced apoptosis in rat hepatocytes primary cultures. Toxicol Appl Phramacol 2000;163:209–20.

[29] Brigotti M, Alfieri R, Sestili P, Bonelli M, Petronini PG, Guidarelli A, et al. Damage to nuclear DNA induced by Shiga toxin 1 and ricin in human endothelial cells. FASEB J 2002;16:365–72.

[30] Armstrong JS, Steinauer KK, Hornung B, Irish JM, Lecane P, Birrell GW, et al. Role of glutathione depletion and reactive oxygen species generation in apoptosis signalling in a human lymphoma cell line. Cell Death Differ 2002;9:252–63.

[31] Janicke RU, Sprengart ML, Wati MR, Porter AG. Caspase-3 is required for DNA fragmentation and morphological changes associated with apoptosis. J Biol Chem 1998;273:935–60.

[32] Fisher U, Janicke RU, Schulz-Osthof K. Many cuts to ruin: a comprehensive update of caspase substrates. Cell Death Differ 2003;10:76–100.

[33] Gan YH, Peng SQ, Liu HY. Molecular mechanism of apoptosis induced by ricin in HeLa cells. Acta Pharmacol Sin 2000;21:243–8.

[34] Liu X, Zou H, Slaughter C, Wang X. DFF, a heterodimeric protein that functions downstream of caspase-3 to trigger DNA fragmentation during apoptosis. Cell 1997;89:175–84.

[35] Enari M, Sakahira H, Yokoyama H, Okkawa K, Iwamastsu A, Nagata S. A caspase-activated DNAse that degrades DNA during apoptosis, and its inhibitor ICAD. Nature 1998;391:43–50.

[36] Halenbeck R, MacDonald H, Roulston A, Chen TT, Conroy L, Williams LT. CPAN, a human nuclease regulated by the caspase-sensitive inhibitor DFF45. Curr Biol 1998;8:537–40.

[37] Laszlo V, Szabo C. The therapeutic potential of poly(ADP-ribose) polymerase inhibitors. Pharmacol Rev 2002;54:375–429.

[38] Boulares AH, Zoltoski AJ, Sherif ZA, Yakovlev A, Smulson ME. Roles of DNA fragmentation factor and poly(ADP-ribose)polymerase-1 in sensitisation of fibroblasts to tumour necrosis factor-induced apoptosis. Biochem Biophys Res Commun 2002;290:796–801.